A control volume approach to parameterise environmental effects of floating offshore wind platforms

Author Names: **Emma C Edwards**, Takafumi Nishino, Christopher Vogel, Deborah Greaves
Department of Engineering Science, University of Oxford, Oxford, United Kingdom
emma.edwards@eng.ox.ac.uk

1 INTRODUCTION

Evaluating the environmental impacts of floating offshore wind represents a key research priority within the floating wind sector [1]. An important first step is to parameterise the hydrodynamic effect of floating offshore wind turbine (FOWT) platforms, with the aim of incorporating the parameterisation into larger ocean-scale models.

Parameterising floating wind farms to use in coupled atmosphere-ocean models is an area of active research. However, most work has focused on parameterising the wind turbine, rather than the platform. The closest related studies include Deng et al. [2], who model the influence of floating wind farms on surface waves and roughness in regional atmospheric models, and Martini et al. [3], who examine the effects of metocean conditions on floating wind farm power production.

This abstract presents an initial modelling framework for parameterising the environmental effects of FOWT platforms, as a first step toward implementation in ocean models (e.g. FVCOM). We analyse a simplified control volume (Figure 1) surrounding a floating platform subjected to a uniform steady current and a single incident progressive wave. Using a control-volume approach, we quantify the relative magnitudes of the governing terms in the momentum conservation equation across multiple current speeds, identifying the terms that dominate the momentum balance, using the VolturnUS-S [4] semi-submersible as a representative platform.

2 CONTROL VOLUME ANALYSIS Consider the 2D control volume shown in Figure 1. The control volume is defined to be the fluid surrounding the floating wind platform (shown in yellow), extending to the ocean floor, and extending outward a distance R in front of and behind the platform. In this initial analysis, we assume deep water ($d = 200\,\mathrm{m}$) and small amplitude waves ($A = 1\,\mathrm{m}$). We assume that there is a known uniform and steady horizontal current, at $x = -R$, with speed U_∞.

2.1 Current-only We first perform a control volume analysis for the case of no incident or scattered waves, with a current only. We assume the downstream velocity is piecewise constant, with $U = U_1$ from $z = 0$ to $z = -h$ (where h is the draft of the FOWT platform) and $U = U_2$ from $z = -h$ to $z = -d$. We assume drag force on the FOWT platform is given by $F_{VD} = (C_q/b)U_\infty^2$ in the surge direction, where $C_q = (0.5 C_D \rho A_p)$, C_D is drag coefficient, and A_p is frontal projected area, and b is the beam of the platform ($b = 90.13\,\mathrm{m}$), because our system is 2D. We use the C_q value given by the VolturnUS-S platform reference document [4] (calculated via CFD simulations of the platform moving with unit horizontal

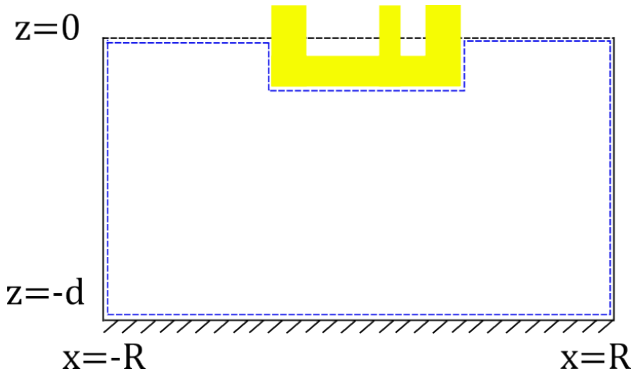

Figure 1: 2D Control volume surrounding the floating platform

fluid velocity). Assuming an incompressible and inviscid (other than the F_{VD} term) fluid and using conservation of mass and momentum, we can solve for U_1 and U_2:

$$U_1 = \frac{U_\infty d - U_2(d-h)}{h}, \qquad U_2 = U_\infty + \sqrt{\frac{(C_q/b)hU_\infty^2}{d(d-h)\rho}}. \tag{1}$$

2.2 Wave and current We next extend the control volume analysis to the combined wave-current case by introducing a single incident progressive wave and averaging over one wave period. Here, we assume the fluid is incompressible and inviscid except for a parametrised viscous drag force acting on the platform, so linear potential flow theory is used for wave terms. This simplification is justified since high computational efficiency is critical for implementation within an ocean model. Momentum flux can occur only through the two boundary surfaces at $x = -R$ and $x = R$. Velocity can be expressed as $u = u_w(x, z, t) + U(x, z)$ where u_w is the velocity due to waves, and $U(x, z)$ is velocity due to current, which we assume is not a function of time. $\frac{\partial \rho}{\partial t} = 0$ and $\overline{u_w} = 0$, and we assume there are no body forces in the x-direction. Averaging over one wave period, dynamic pressure contributions vanish and hydrostatic pressure cancels between control surfaces, leaving only the hydrodynamic force on the platform, $F_{P,x}$. Therefore, conservation of momentum in the x-direction is

$$\overline{\rho \int_{-d}^{0} [u(x=-R,z)]^2 dz} - \overline{\rho \int_{-d}^{0} [u(x=R,z)]^2 dz} + \overline{F_{P,x}} = 0. \tag{2}$$

Of the components of $F_{P,x}$, only the viscous drag term, F_{VD}, has a non-zero mean over one wave period. This term is modelled using a Morison-type formulation in section 2.3. Using potential flow theory, we express the advective momentum flux terms as

$$\overline{\rho \int_{-d}^{0} [u_w(x=\mp R,z) + U]^2 dz} = \begin{cases} \frac{\rho}{4k} a_{w,U}^2 (1 - e^{-2kd}) + \rho d U_\infty^2 \\ \frac{\rho}{4k} a_{w,D}^2 (1 - e^{-2kd}) + \rho (h U_1^2 + (d-h) U_2^2) \end{cases} \tag{3}$$

where k is wavenumber obtained from the deep-water dispersion relation with current $(\omega - kU)^2 = gk$ and $a_{w,U}$ and $a_{w,D}$ are the complex amplitudes of the wave velocity at $x = \mp R, z = 0$. Here, we assume the downstream mean current profile is unchanged by the presence of waves, so U_1 and U_2 are assumed to be the same as the current-only case.

2.3 Morison-type drag We can express the viscous drag term (in the wave and current case) as a 'Morison-type' drag force for the moving body:

$$F_{VD,x} = C_q|u - \dot{\Xi}_1|(u - \dot{\Xi}_1) \tag{4}$$

where Ξ_1 is the surge displacement of the platform. Since C_q is given for the whole platform, we choose the fluid velocity at $z = -h/2$. We assume $u = u_w + U_\infty$ at the body, and we can express $u_w = Re\{a_w e^{i\omega t}\}$, where $a_w = |a_w|e^{i\psi_w}$, and $\Xi_1 = Re\{\xi_1 e^{i\omega t}\}$, where $\xi_1 = |\xi_1|e^{i\psi_1}$. Labelling $a_r = a_w - \xi_1$, we get

$$\overline{|u - \dot{\Xi}_1|(u - \dot{\Xi}_1)} = \begin{cases} \frac{1}{2}\left(|a_r|^2 + 2U_\infty^2\right) & |a_r| < U_\infty \\ \frac{1}{\pi}\left[(|a_r|^2 + 2U_\infty^2)\sin^{-1}\left(\frac{U_\infty}{|a_r|}\right) + 3U_\infty\sqrt{|a_r|^2 - U_\infty^2}\right] & |a_r| \geq U_\infty. \end{cases} \tag{5}$$

2.4 Implementation We use the boundary-element-method code PyHAMS [5], which outputs pressure for specified field points. To find a_w, we use $a_w = \hat{p}k/(\rho\omega_1)$, where $\hat{p}$ is the complex amplitude of output pressure at $x = \pm R, z = 0$. Here ω_1 denotes the intrinsic frequency, while all time-harmonic quantities are expressed using absolute frequency ω. To find $|\xi_1|$, we use PyHAMS to get the hydrodynamic coefficients for each ω_1 and then use $\xi = Z^{-1}X$, where $Z = -\omega_1^2(M + A) - i\omega_1 B + (C_h + C_m)$, where M is the mass matrix, A is the added mass matrix, B is the radiation damping matrix, C_h is the hydrodynamic stiffness matrix, and C_m is the linearised mooring stiffness matrix, and X is the excitation force vector. C_h, C_m and M are found using frequency-domain FOWT dynamic solver RAFT [6].

3 RESULTS AND DISCUSSION To quantify the effect of the platform and assess the relative importance of the terms in the momentum balance, Figure 2 shows the change in each of the five momentum-balance terms resulting from the inclusion of the platform, relative to the no-platform case. For the latter, we assume $u_w(x, z, t) = u_I(x, z, t)$ (incident wave velocity) and $U = U_\infty$ everywhere. Changes in momentum flux are denoted by Δ_F, with subscripts U and D indicating upstream and downstream boundaries, respectively. All terms are nondimensionalised by $(\rho U_\infty^2 h)$, denoted by prime ($'$), and are shown as functions of kL, where k is wavenumber and L is length of the platform in the x-direction ($L = 90.3\,\mathrm{m}$). We consider two values of inflow current speed: $U_\infty = 0.05\,\mathrm{m/s}$ (representing a low-speed current) and $U_\infty = 0.5\,\mathrm{m/s}$ (representing a high-speed current).

For the low-speed case (Figure 2a), the upstream change in wave-induced momentum flux, $\Delta'_{F_U,w}$, oscillates about zero, consistent with constructive and destructive interference between incident and scattered wave fields. In contrast, the downstream change, $\Delta'_{F_D,w}$, remains generally negative suggesting additive contribution of these components. Both $\Delta'_{F_D,w}$ and the viscous drag force, F'_{VD}, exhibit similar trends with opposite signs, peaking near $kL = 3$ and suggesting enhanced wave scattering and platform motion. For this weak-current case, momentum-flux changes associated with the current are small. Figure 2b shows that in the high-speed current case the viscous drag term and the downstream current-induced momentum change dominate. The wave-induced momentum-flux terms retain similar trends to the low-current case but are comparatively small.

This new approach has the potential to enable efficient parameterisation of hydrodynamic impacts of FOWT platforms in ocean models (e.g. FVCOM) for general configurations,

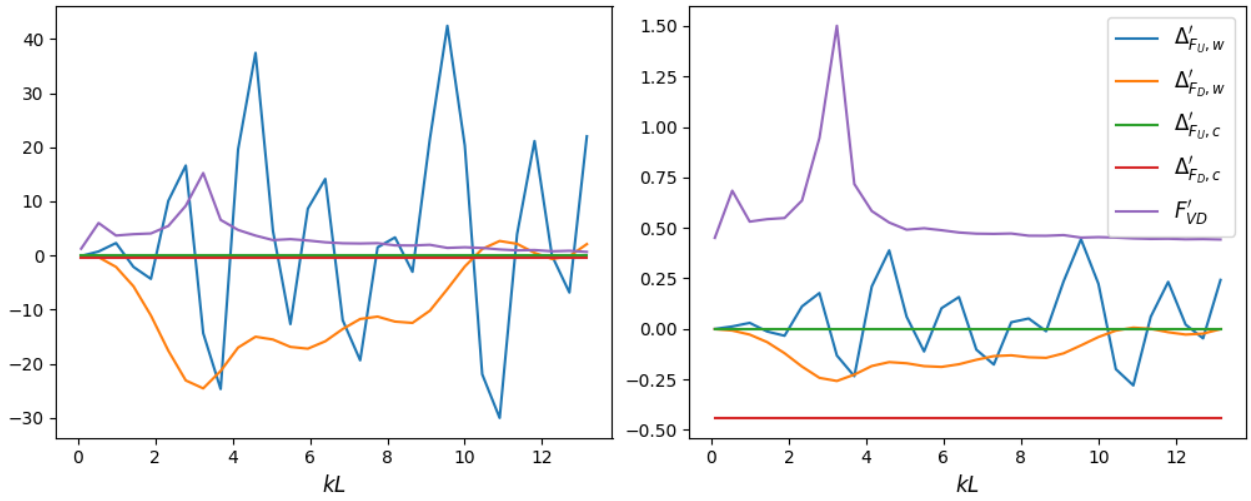

Figure 2: Nondimensionalised change in wave momentum flux relative to the no-platform case at upstream (blue) and downstream (orange) boundaries; change in current momentum flux at upstream (green) and downstream (red) boundaries, and drag force (purple) for a) $U_\infty = 0.05\,\mathrm{m/s}$ and b) $U_\infty = 0.5\,\mathrm{m/s}$

requiring only BEM-derived hydrodynamic coefficients and an overall drag coefficient C_D. The resulting computational efficiency allows for rapid ocean model simulations that can be coupled with ecological models, allowing wind farm developers to assess environmental impacts more easily. In future work, we will incorporate mooring forces analogously to Morison-type viscous forces (equation 4) and mean drift forces, using updated C_D values from more relevant high-fidelity simulations. We will also integrate over the wave spectrum to express the parameterisation in terms of spectral quantities available in ocean wave models, and validate the approach against high-fidelity simulations to assess its range of applicability.

REFERENCES

[1] Maxwell, S. M., Kershaw, F., Locke, C. C., Conners, M. G., Dawson, C., Aylesworth, S., Loomis, R., and Johnson, A. F. 2022. *Potential impacts of floating wind turbine technology for marine species and habitats.* Journal of Environmental Management 307.

[2] Deng, S., Yang, S., Chen, S., Chen, D., Yang, X., and Cui, S. 2024. *A parameterization scheme for the floating wind farm in a coupled atmosphere–wave model (COAWST v3. 7).* Geoscientific Model Development 17(12), 4891–4909.

[3] Martini, M., Guanche, R., Armesto, J. A., Losada, I. J., and Vidal, C. 2016. *Met-ocean conditions influence on floating offshore wind farms power production.* Wind Energy 19(3), 399–420.

[4] Allen, C., Viscelli, A., Dagher, H., Goupee, A., Gaertner, E., Abbas, N., Hall, M., and Barter, G. 2020. Definition of the UMaine VolturnUS-S reference platform developed for the IEA wind 15-megawatt offshore reference wind turbine. Tech. rep., National Renewable Energy Lab.(NREL).

[5] NLRWindSystems. pyhams. `https://github.com/NLRWindSystems/pyHAMS`. Accessed: 2026-01-14.

[6] Hall, M., Housner, S., Zalkind, D., Bortolotti, P., Ogden, D., and Barter, G. An open-source frequency-domain model for floating wind turbine design optimization. In Journal of physics: Conference series (2022), IOP Publishing.